doi:10.1093/scan/nst064 SCAN (2014) 9, 900–908

Ventromedial prefrontal cortex and the regulation of physiological arousal

Sheng Zhang,[1] Sien Hu,[1] Herta H. Chao,[2,3] Jaime S. Ide,[4] Xi Luo,[5] Olivia M. Farr,[6] and Chiang-shan R. Li[1,6,7]
[1]Department of Psychiatry, [2]Department of Medicine, Yale University, New Haven, CT 06519, USA, [3]Department of Medicine, VA Connecticut Healthcare Systems, West Haven, CT 06516, USA, [4]Department of Science and technology, University Federal De Sao Paulo, Sao Jose Dos Campos, Brazil, [5]Department of Biostatistics and Center for Statistical Sciences, Brown University, Providence, Rhode Island 02912, USA, [6]Interdepartmental Neuroscience Program, and [7]Department of Neurobiology, Yale University, New Haven, CT 06520, USA

Neuroimaging studies show a correlation between activity of the ventromedial prefrontal cortex (vmPFC) and skin conductance measurements. However, little is known whether this brain region plays a causal role in regulating physiological arousal. To address this question, we employed Granger causality analysis (GCA) to establish causality between cerebral blood oxygenation level-dependent and skin conductance signals in 24 healthy adults performing a cognitive task during functional magnetic resonance imaging. The results showed that activity of the vmPFC not only negatively correlated with skin conductance level (SCL) but also Granger caused SCL, thus establishing the direction of influence. Importantly, across participants, the strength of Granger causality was negatively correlated to phasic skin conductance responses elicited by external events during the behavioral task. In contrast, activity of the dorsal anterior cingulate cortex positively correlated with SCL but did not show a causal relationship in GCA. These new findings indicate that the vmPFC plays a causal role in regulating physiological arousal. Increased vmPFC activity leads to a decrease in skin conductance. The findings may also advance our understanding of dysfunctions of the vmPFC in mood and anxiety disorders that involve altered control of physiological arousal.

Keywords: ventromedial prefrontal cortex; arousal; skin conductance; Granger causality

INTRODUCTION

Changes in physiological arousal accompany attention, decision-making, affective regulation and other motivated behaviors (Frith and Allen, 1983; Damasio, 1994; Bechara *et al.*, 1997; Critchley, 2002, 2009; Dolan, 2002). Skin conductance, which increases via sympathetic innervations of the sweat glands, is often used as a physiological index of arousal (Critchley, 2002; Naqvi and Bechara, 2006). Skin conductance comprises a tonic and phasic component. Tonic skin conductance, or skin conductance level (SCL), reflects the overall conductivity of the skin over a long period of time; in contrast, the phasic component—skin conductance response (SCR)—refers to a discrete and short fluctuation in skin conductance, as elicited by a cognitive event. Numerous imaging studies have investigated the neural correlates of SCL and SCR.

The medial prefrontal cortex, including anterior cingulate cortex (ACC) and ventromedial prefrontal cortex (vmPFC), is consistently involved in cerebral responses to physiological arousal (Table 1). For instance, in a decision-making task, activity of the dorsal ACC (dACC) was positively modulated by the SCR during a delay period between reward-related decisions and their outcomes (Critchley *et al.*, 2001). In contrast, the vmPFC showed task independent negative correlations with the SCL. When participants controlled their arousal via biofeedback by increasing SCL during an arousal condition while decreasing SCL during a relaxation condition, vmPFC activity was negatively correlated with SCL in both conditions (Nagai *et al.*, 2004). A recent study demonstrated that the negative correlation between the vmPFC activity and SCL also occurs during resting sate (Fan *et al.*, 2012). It has been postulated that while the dACC responds to changes in skin conductance, the vmPFC may play a role in regulating physiological arousal (Damasio, 1994; Critchley *et al.*, 2000, 2001).

However, the results of these earlier studies were based on correlation and it is not clear whether the vmPFC plays a direct role in regulating physiological arousal. Elucidation of this relationship is critical to our understanding of the functions and dysfunctions of vmPFC and the etiologies of mood and anxiety disorders that implicate altered emotional regulation. We sought to address this issue by examining the causal relationship between cerebral activities and skin conductance with Granger causality analysis (GCA; Granger, 1969). In functional magnetic resonance imaging (fMRI), GCA has been widely used to investigate the causal relationship between regional activities during cognitive performance (Ding *et al.*, 2006; Stilla *et al.*, 2007; Deshpande *et al.*, 2008, 2009; Duann *et al.*, 2009). For instance, a recent study employed GCA to elucidate the flow of information between ventral and dorsal attention networks during a trial-by-trial cued visual spatial attention task (Wen *et al.*, 2012). Here, GCA would be a useful tool to explore the casual relationship between cerebral activity and skin conductance, two time series recorded continuously throughout a cognitive task. We hypothesized that blood oxygenation level-dependent (BOLD) signals of the vmPFC would not only correlate negatively with but also Granger cause SCL. Furthermore, the strength of causality or regulatory influence of the vmPFC would negatively correlate with events-evoked SCR across subjects.

MATERIALS AND METHODS

Subjects and behavioral tasks

Twenty-four adult healthy subjects (10 males, 30 ± 11 years of age, all right-handed and using their right hand to respond) participated in this study. All participants denied medical including neurological illnesses, history of head injuries, current use of any medications or use of any psychotropic medications in the past year. They were also free of any psychiatric diagnoses as assessed with the Structured Clinical Interview for Diagnostic and Statistical Manual Disorders (First

Received 19 February 2013; Accepted 20 April 2013
Advance Access publication 24 April 2013

The authors thank Sarah Bednarski and Emily Erdman in subject recruitment and assessment as well as running of some of the imaging studies. This work was supported by National Institute of Health grants R01DA023248, R21AA018004, K02DA026990, R03CA138121, Tourette Syndrome Association, William O. Seery Foundation and a Yale Cancer Center translational pilot grant. The content is solely the responsibility of the authors and does not necessarily represent the official views of the National Institute of Health.

Correspondence should be addressed to Sheng Zhang, Connecticut Mental Health Center S103, Department of Psychiatry, Yale University School of Medicine, 34 Park Street, New Haven, CT 06519, USA. E-mail: sheng.zhang@yale.edu

Table 1 A summary of brain regions within the medial prefrontal cortex that respond to skin conductance signals

Study	MNI coordinate (mm)			Identified region and approximate Brodmann area (BA)
	x	*y*	*z*	
Decision making task (Critchley *et al.*, 2000)				
Activity preceding SCR	−12	50	10	Rostral ACC; BA 10
Activity subsequent to SCR	10	52	−10	vmPFC; BA 10
Decision making task (Critchley *et al.*, 2001)				
Positive correlation with SCR	4	32	24	Dorsal ACC; BA 32
Biofeedback relaxation task (Nagai *et al.*, 2004)				
Positive correlation with SCL	−12	32	36	Dorsal ACC; BA 32
Negative correlation with SCL	−2	58	−10	vmFPC; BA 11
Emotional faces viewing task (Williams *et al.*, 2005)				
Activation for fear and SCR	14	42	7	Rostral ACC; BA 32
Activation for anger and SCR	7	31	28	Dorsal ACC; BA 32
	7	28	−7	vmPFC; BA 11
Activation for disgust and SCR	11	20	21	Dorsal ACC; BA 32
Resting state (Fan *et al.*, 2012)				
Positive correlation with SCL	6	6	44	Dorsal ACC; BA 24
Negative correlation with SCL	2	28	−18	vmPFC; BA 11

et al., 1995), denied use of illicit substances and showed a negative urine toxicology test on the day of fMRI. All subjects were paid to participate and signed a written consent after details of the study were explained, in accordance to institute guidelines and procedures approved by the Yale Human Investigation Committee.

We employed a simple reaction time (RT) task in this stop-signal paradigm, as described in details in our previous studies (Chao *et al.*, 2009; Li *et al.*, 2009; Zhang and Li, 2012a). Briefly, there were two trial types: 'go' (∼75%) and 'stop' (∼25%), randomly intermixed. A small dot appeared on the screen to engage attention at the beginning of a go trial. After a randomized time interval (fore-period) between 1 and 5 s, the dot turned into a circle, prompting the subjects to quickly press a button. The circle vanished at button press or after 1 s had elapsed, whichever came first, and the trial terminated. A premature button press prior to the appearance of the circle also terminated the trial. In a stop trial, an additional 'X', the 'stop' signal, appeared after the go signal and instructed the subjects to withhold button press. Likewise, a trial terminated at button press or after 1 s had elapsed. There was an inter-trial-interval of 8 s to allow adequate spacing between events of interest and identification of SCR associated with these events. The time interval between go and stop signals or stop signal delay (SSD) started at 200 ms and varied from one stop trial to the next according to a staircase procedure, increasing and decreasing by 64 ms, each after a successful and failed stop trial (Levitt, 1971; De Jong *et al.*, 1990). With the staircase procedure, a 'critical' SSD could be computed that represents the time delay required for the subject to succeed in half of the stop trials (Levitt, 1971). Subjects were instructed to respond to the go signal quickly while keeping in mind that a stop signal could come up in a small number of trials. With the staircase procedure, we anticipated that the subjects would succeed in withholding their response in approximately half of the stop trials. Prior to the fMRI study, each subject had a practice session outside the scanner. Each subject completed six 10 min runs of the task. Across 24 subjects, we had an average of 205 ± 14 go and 69 ± 7 stop including 38 ± 4 stop success and 31 ± 4 stop error trials.

Skin conductance acquisition and analysis

With a Biopac MP150 system, skin conductance was continuously recorded during fMRI from the palmer surfaces of the index and middle fingers of the left hand. The biopac system used a AcqKnowledge 4.1 software (Biopac Systems, USA) and the Biopac electrodermal activity amplifier module (Galvanic Skin Response 100c) set at a channel sampling rate of 31 Hz and a gain of 5 μSiemens (μS) per volt (resulting in a resolution of 0.0015 μS). Recording of skin conductance is synchronized with behavioral task and image acquisition. A smoothing function with a moving average of 500 ms was applied in order to eliminate high-frequency noise (Figner and Murphy, 2011). The SCL was computed by resampling the skin conductance waveform to match the TR (2 s) used in the functional imaging data acquisition and analysis (Critchley *et al.*, 2000; Patterson *et al.*, 2002). Because all trials were longer than 10 s, we used a 10 s window aligned with go signal onset to compute the SCR associated with each trial. Thus, the SCR of each trial was computed as the onset-to-peak amplitude difference in skin conductance in this 10 s window as in a previous study (Zhang *et al.*, 2012).

Imaging protocol

Conventional T1-weighted spin echo sagittal anatomical images were acquired for slice localization using a 3T scanner (Siemens Trio). Anatomical images of the functional slice locations were next obtained with spin echo imaging in the axial plane parallel to the AC–PC line with TR = 300 ms, TE = 2.5 ms, bandwidth = 300 Hz/pixel, flip angle = 60°, field of view = 220 × 220 mm, matrix = 256 × 256, 32 slices with slice thickness = 4 mm and no gap. Functional, BOLD signals were then acquired with a single-shot gradient echo echoplanar imaging (EPI) sequence. Thirty-two axial slices parallel to the AC–PC line covering the whole brain were acquired with TR = 2000 ms, TE = 25 ms, bandwidth = 2004 Hz/pixel, flip angle = 85°, field of view = 220 × 220 mm, matrix = 64 × 64, 32 slices with slice thickness = 4 mm and no gap.

Imaging data preprocessing

Brain imaging data were preprocessed using Statistical Parametric Mapping version 8 (Wellcome Department of Imaging Neuroscience, University College London, UK). Images from the first five TRs at the beginning of each session/run were discarded to enable the signal to achieve steady-state equilibrium between RF pulsing and relaxation. Images of each individual subject were first corrected for slice timing and realigned (motion corrected). A mean functional image volume was constructed for each subject for each run from the realigned image

volumes. These mean images were normalized to an Montreal Neurological Institute (MNI) EPI template with affine registration followed by non-linear transformation (Ashburner and Friston, 1999). The normalization parameters determined for the mean functional volume were then applied to the corresponding functional image volumes for each subject. Finally, images were smoothed with a Gaussian kernel of 8 mm at full width at half maximum.

Additional preprocessing was applied to reduce spurious BOLD variances that were unlikely to reflect neuronal activity (Fox *et al.*, 2005; Zhang and Li, 2012b). The sources of spurious variance were removed through linear regression by including the signal from the ventricular system, the white matter and the whole brain, in addition to the six parameters obtained by rigid body head motion correction. First-order derivatives of the whole brain, ventricular and white matter signals were also included in the regression.

Linear correlation with skin conductance

We computed for individual subjects the correlation coefficient between the SCL and the time courses of each voxel for the whole brain. Note that the skin conductance impulse response function is very close in shape and latency to that of the canonical hemodynamic response function (HRF) (Patterson *et al.*, 2002; Nagai *et al.*, 2004). Thus, SCL could be cross correlated with BOLD signals without additional processing. We then converted these individual correlation maps, which were not normally distributed, to z score maps by Fisher's z transform (Charles F. Bond and Richardson, 2004): $z = 0.5 \log_e[(1 + r)/(1 - r)]$. The z maps were used in the second-level random effects analysis (Penny *et al.*, 2004). A one-sample t-test was applied to the 'z maps' across 24 subjects to identify regional activities correlated to skin conductance.

In region of interest (ROI) analysis, we used MarsBar (http://marsbar.sourceforge.net/) to derive for each individual subject the effect size of activity change for the ROIs. Functional ROIs were defined based on activated clusters from whole-brain analysis. All voxel activations were presented in MNI coordinates.

Granger causality analysis

BOLD and skin conductance signals were examined with GCA (Granger, 1969), which has been widely used to describe 'causal' influence between sets of EEG or fMRI time series (Ding *et al.*, 2000; Roebroeck *et al.*, 2005; Abler *et al.*, 2006; Stilla *et al.*, 2007; Deshpande *et al.*, 2008; Sato *et al.*, 2009; Wen *et al.*, 2012), as described in details in our previous studies (Duann *et al.*, 2009; Ide and Li, 2011a, 2011b). Briefly, we used multivariate autoregressive (MAR) modeling (Harrison *et al.*, 2003; Sato *et al.*, 2009) to perform GCA. In an unrestricted model of the BOLD time series

$$Y(t) = \sum_{i=1}^{p} A_i Y(t - i) + \varepsilon(t),\ t = 1,2,\ldots,T, \tag{1}$$

$Y(t)$ is a column vector $[y_1(t),y_2(t),\ldots,y_n(t)]$ in which each element $y_j(t), j = 1,2,\ldots,n$, is the average time series of a ROI at time point t; T is the number of time points; n is the number of ROIs and $\varepsilon(t)$ is a column vector $[\varepsilon_1(t),\varepsilon_2(t),\ldots,\varepsilon_n(t)]$ of residuals at time point t. The model order is represented by p and A_i is a n-by-n matrix given by

$$A_i = \begin{bmatrix} a_{11}^{(i)} & a_{12}^{(i)} & \cdots & a_{1n}^{(i)} \\ a_{21}^{(i)} & a_{22}^{(i)} & \cdots & a_{2n}^{(i)} \\ \vdots & \vdots & \ddots & \vdots \\ a_{n1}^{(i)} & a_{n2}^{(i)} & \cdots & a_{nn}^{(i)} \end{bmatrix}, \quad i = 1,2,\ldots,p, \tag{2}$$

estimated by ordinary least squares (Seth, 2010). To determine the model order, we employed the Bayesian Information Criterion (Schwarz, 1978; Gentle *et al.*, 2004). The application of MAR modeling required that each ROI or SCL was covariance stationary, which we examined with the Augmented Dickey Fuller (ADF) test (Hamilton, 1994). The ADF test verified that there was no unit root in the modeled time series. To test whether variable x Granger causes y, where $x,y \in Y(t), x \neq y$, we computed the regression equation (1) without variable x (the restricted model) and obtained the residual sum of squares RSS_r of variable y. The residual sum of squares of y is given by $\mathrm{RSS} = \sum_{t=1}^{T} (y(t) - \hat{y}(t))^2 = \sum_{t=1}^{T} \varepsilon(t)^2$, where $\hat{y}$ represents the predicted value of y. These residuals were used to compute the Granger causality strength measures (F-values) of each possible connection between ROIs and skin conductance (Hamilton, 1994):

$$F = \frac{(\mathrm{RSS_r} - \mathrm{RSS_{ur}})/p}{\mathrm{RSS_{ur}}/(T - 2p - 1)}, \tag{3}$$

where $\mathrm{RSS_{ur}}$ is the residual sum of squares of variable y in the unrestricted model. We tested the significance of the Granger causality between time series by an F test and used binomial test to assess statistical significance in group analysis as described in details earlier (Duann *et al.*, 2009; Ide and Li, 2011a, 2011b). For each connection, we counted the number of subjects that had significant connections and estimated its significance using a binomial distribution with parameters $n = 24$ trials, and $P = q = 0.5$ (same probability to observe a connection or not). For each subject, we had a total of 1770 (295×6) time points for GCA.

To assess how the strength of Granger causality relate to event-evoked arousal, we examined the correlation across subjects between the causality strength measures (F-values) and stimulus-evoked SCR with a linear regression.

RESULTS

Behavioral performance and SCRs

Behavioral results of the SST are listed in Table 2(a). Participants succeeded in about half of the stop trials, indicating the success of the staircase procedure in tracking their performance.

SCRs during the SST are shown in Table 2(b). As described in the 'Materials and Methods' section, we quantified the change of skin conductance or SCR by subtracting the amplitude at the baseline from the amplitude at the peak in a 10 s window after stimulus onset for each trial. Across all 24 subjects, go (G), stop success (SS) and stop error (SE) trials showed significant differences in SCR ($P = 0.003$, one-way ANOVA), as did planned comparisons: G *vs* SS ($P = 0.01$), G *vs* SE ($P = 0.0002$) and SS *vs* SE ($P = 0.0003$), with two-sample t-tests.

Arousal related brain activation

We computed for individual subjects the correlation coefficient between the SCL and the time courses of each voxel for the whole brain, and normalized these correlation maps with Fisher's z transformation for a one-sample t-test (see 'Materials and Methods' section). The ACC as well as right superior frontal gyrus showed significant (cluster level $P < 0.05$, corrected for family-wise error or FWE of multiple comparisons) positive correlation, whereas the vmPFC showed significant (cluster level $P < 0.05$, FWE corrected) negative correlation, with skin conductance (Figure 1 and Table 3). This activity of the ACC and vmPFC did not correlate across subjects ($P > 0.1$).

Table 2 Behavioral performance and trial-specific SCR

a. General performance in the stop signal task

Go RT (ms)	Coefficient of variation in go RT	% go	% stop	SSRT (ms)	Critical SSD (ms)	Post-error slowing (effect size)
641 ± 74	0.21 ± 0.04	94.3 ± 6.5	55.3 ± 3.5	235 ± 42	411 ± 77	1.78 ± 1.29

b. SCR of go, stop, stop success and stop error trials

	Go	Stop	Stop success	Stop error
SCR (μSiemens)	0.16 ± 0.18	0.33 ± 0.34	0.22 ± 0.22	0.49 ± 0.51

Note: %go and %stop, percentage of successful go and stop trials; RT, reaction time; SSRT, stop-signal reaction time; SSD, stop signal delay; all numbers are mean ± s.d.

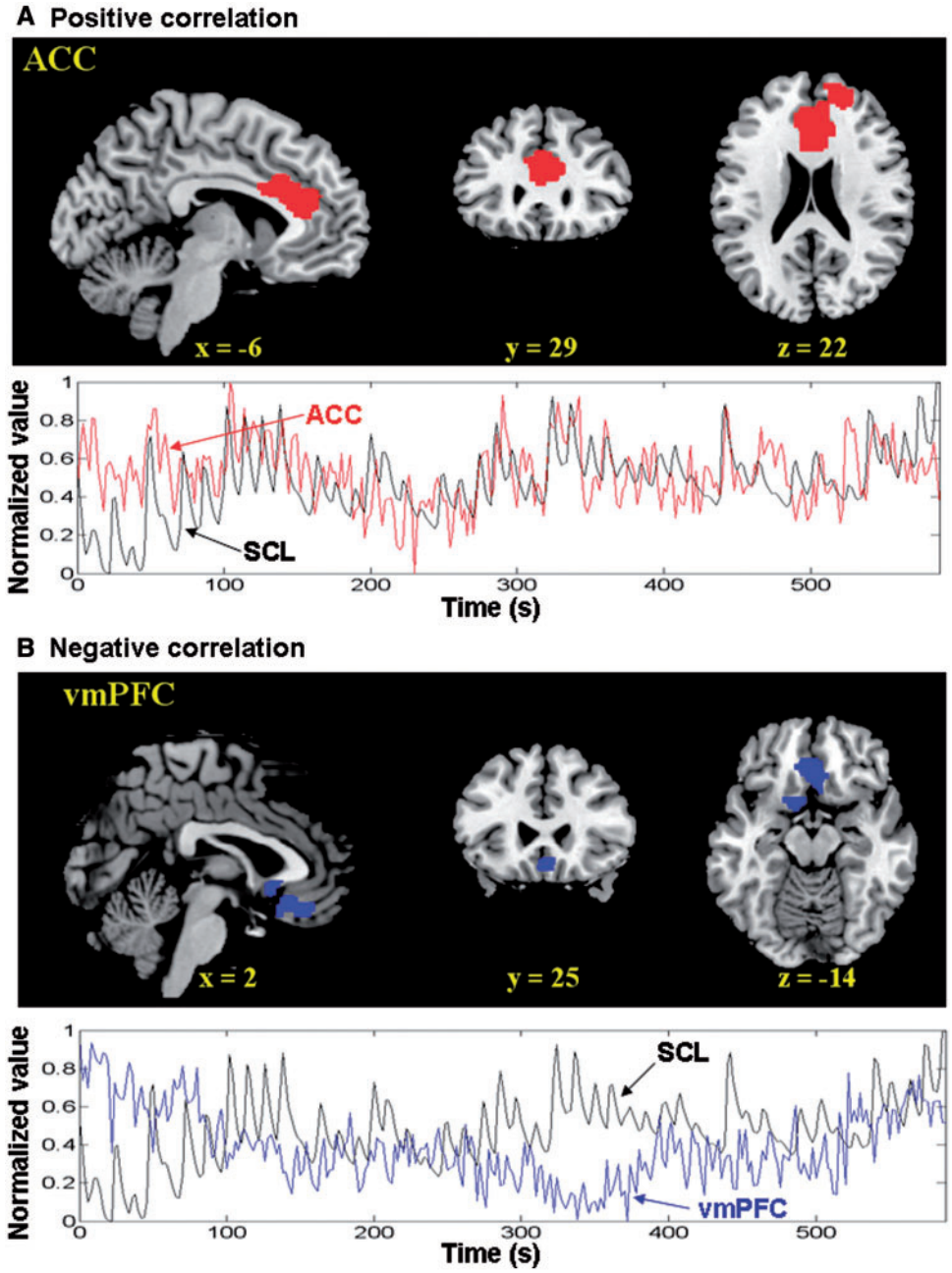

Fig. 1 Brain regions showed positive (top of **A**) and negative (top of **B**) correlations with the SCL across 24 subjects at voxel $P < 0.0001$ uncorrected and cluster $P < 0.05$ corrected for FWE of multiple comparisons. (Bottom of A and B) Data from a typical participant show that the time series of the ACC and vmPFC are each correlated and anti-correlated with SCL in a 10 min session.

Table 3 Brain regions showing significant correlations with skin conductance time series (voxel $P < 0.0001$ uncorrected and cluster-level threshold of $P < 0.05$, FWE corrected)

Cluster size (mm^3)	Voxel *z* value	MNI coordinate (mm)			Identified region and approximate Brodmann area (BA)
		X	*y*	*z*	
Positive correlation					
21 222	5.07	−6	29	22	Anterior cingulated cortex; BA 24/32
	4.72	24	59	13	Right superior frontal gyrus; BA 10
Negative correlation					
6372	4.68	3	32	−17	Ventromedial prefrontal cortex; BA 11
	4.49	−12	8	−17	Left olfactory cortex; BA 25

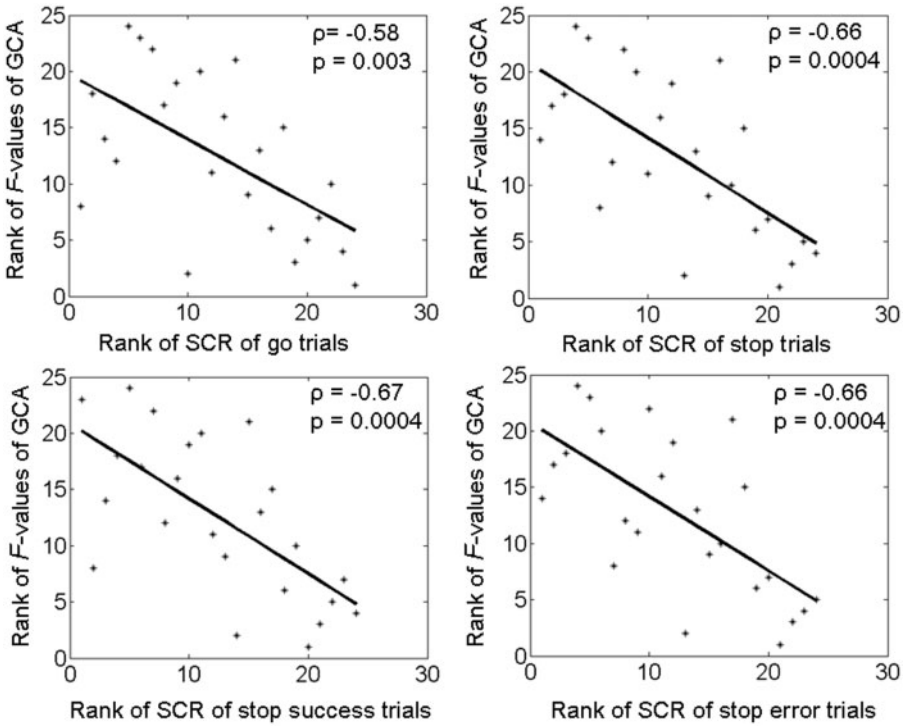

Fig. 2 The strength of Granger causality (*F*-value) of the vmPFC in regulating skin conductance is negatively correlated with SCR elicited by go ($P = 0.003$, $\rho = -0.58$; Spearman regression), stop ($P = 0.0004$, $\rho = -0.66$), as well stop success ($P = 0.0004$, $\rho = -0.67$) and stop error ($P = 0.0004$, $\rho = -0.66$) trials. That is, the stronger the regulatory influence of vmPFC, the less the SCR is elicited. Assuming linearity between the *F*-value and SCR, Pearson regressions also showed significant correlation between the two variables: go ($P = 0.01$, $r = -0.50$); stop ($P = 0.01$, $r = -0.50$); stop success ($P = 0.0098$, $r = -0.52$) and stop error ($P = 0.016$, $r = -0.49$) trials.

Granger causality analysis

The results of GCA showed that BOLD signals of the vmPFC Granger caused the SCL ($P < 0.05$ for individual GCA and $P = 0.03$, binomial test for group analysis), but the SCL did not Granger cause vmPFC activity ($P = 0.08$). In contrast, there was no significant Granger causality between dACC and SCL in either direction ($P = 0.85$ and 0.27). Moreover, individuals varied in the strength of Granger causality as indexed by the *F*-value (mean ± s.d. = 5.0 ± 4.5; range 1.5–18.6). Across the 24 participants, Spearman regressions showed that higher Granger causality strength (*F*-values) of the vmPFC was associated with less SCRs elicited by go ($P = 0.003$, $\rho = -0.58$), stop ($P = 0.0004$, $\rho = -0.66$), stop success ($P = 0.0004$, $\rho = -0.67$) and stop error ($P = 0.0004$, $\rho = -0.66$) trials during the stop signal task (Figure 2).

Because previous studies used a smaller window (0.5–4.5 s) following stimulus onset to compute the event-related SCR (Delgado *et al.*, 2008; Schiller *et al.*, 2008; Nili *et al.*, 2010), we recomputed the SCR by the onset-to-peak amplitude within a 5 s window and reran the regression analysis. The results were similar: significant negative correlations were observed between the Granger causality strength and the SCR elicited by go ($P = 0.0004$, $\rho = -0.66$), stop ($P = 0.0003$, $\rho = -0.68$), stop success ($P = 0.0001$, $\rho = -0.70$) and stop error ($P = 0.0004$, $\rho = -0.67$) trials. Furthermore, to eliminate the confound of individual variability in mean SCL, we removed the mean value of the skin conductance time series before computing the SCR, and reran the regression analysis. The results were similar: significant negative correlations were observed between the Granger causality strength and the SCR elicited by go ($P = 0.0002$, $\rho = -0.69$), stop ($P = 0.0002$, $\rho = -0.69$), stop success ($P = 0.01$, $\rho = -0.50$) and stop error ($P = 0.0001$, $\rho = -0.73$) trials.

DISCUSSION

vmPFC and the regulation of physiological arousal

We showed that activation of a distinct region in the vmPFC is negatively correlated with moment to moment changes in SCL. Importantly, Granger causality analyses demonstrated that activity of the vmPFC Granger causes skin conductance signals, thus establishing

the direction of influence. Furthermore, across the 24 participants, higher Granger causality strength is associated with less SCRs elicited by cognitive events during the stop signal task. These findings confirmed our hypotheses and are important on two fronts. First, extending previous findings of a negative correlation between the vmPFC and SCL, we demonstrated a direct, causal relationship between the activity of the vmPFC and the changes in physiological arousal. Second, the stronger the regulatory influence of the vmPFC, the less the SCRs to cognitive events. Together, these results support a critical role of this ventromedial prefrontal structure in the control of arousal during cognitive performance.

The finding of a significant negative association between vmPFC activity and SCL replicates the results of biofeedback relaxation (Nagai *et al.*, 2004) and resting state (Fan *et al.*, 2012). Studies using paradigms of fear conditioning similarly demonstrated less activity of the vmPFC when participants anticipated an electric shock and exhibited higher SCR than when they did not expect to receive the shock (Milad *et al.*, 2007; Delgado *et al.*, 2008; Schiller *et al.*, 2008). In another study, the vmPFC increased activity when subjects tried to overcome a real-life fear (Nili *et al.*, 2010); the vmPFC activity was enhanced, whereas the SCR was attenuated, as the level of subjective fear increased during the 'overcome' period. The investigators posited that activity of the vmPFC may be related to the inhibition of fear-related arousal, an interpretation supported by our current findings. Together, it appears that the negative association between the vmPFC and skin conductance activity is task independent.

Posterior *vs* anterior vmPFC: responses to SCR and the effects of a lesion

Another consideration is the anatomical location of the vmPFC as implicated in the regulation of arousal. In addition to a negative correlation with SCL, a few studies have shown a positive correlation between activity of the vmPFC and SCR (Critchley *et al.*, 2000; Patterson *et al.*, 2002; Williams *et al.*, 2005). To address this issue, we delineated the anatomical boundary of the vmPFC cluster identified here and those of other studies (Figure 3). Our vmPFC cluster clearly overlapped the regions where activities were negatively associated with SCL (Nagai *et al.*, 2004; Fan *et al.*, 2012). In contrast, activities that showed positive correlations with the SCR were located in the anterior part of the vmPFC (Critchley *et al.*, 2000; Patterson *et al.*, 2002; Williams *et al.*, 2005). Notably, a recent review suggested a functional differentiation between anterior and posterior vmPFC in relation to mood and anxiety disorders (Myers-Schulz and Koenigs, 2012). The posterior vmPFC was thought to be associated with negative affect and mood (Simpson *et al.*, 2001; Zald *et al.*, 2002; Paradiso *et al.*, 2003; Masten *et al.*, 2009), whereas the anterior vmPFC was associated with positive affect and related emotional states (Somerville *et al.*, 2006, 2010; Gianaros *et al.*, 2007; Glascher *et al.*, 2009; Kim *et al.*, 2010). Patients with major depression exhibit increased posterior vmPFC activity but decreased anterior vmPFC activity (Drevets *et al.*, 1997; Mayberg *et al.*, 2005; Greicius *et al.*, 2007), a pattern of response that reversed after successful treatment (Mayberg *et al.*, 2000, 2005; Kennedy *et al.*, 2007). Thus, it is important to distinguish the exact locales of activity when associating vmPFC with the regulation of arousal and emotion.

The current findings also need to be considered along with lesion studies that implicated the vmPFC in the generation of arousal (Damasio *et al.*, 1990, 1991; Damasio, 1994; Tranel and Damasio, 1994; Zahn *et al.*, 1999). Patients with lesions in the vmPFC have deficits in generating electrodermal responses and showed a reduction in anticipatory arousal, which is the opposite of what would be expected if the vmPFC down-regulates arousal. A possible explanation is that the lesions examined in these studies encompass a much larger

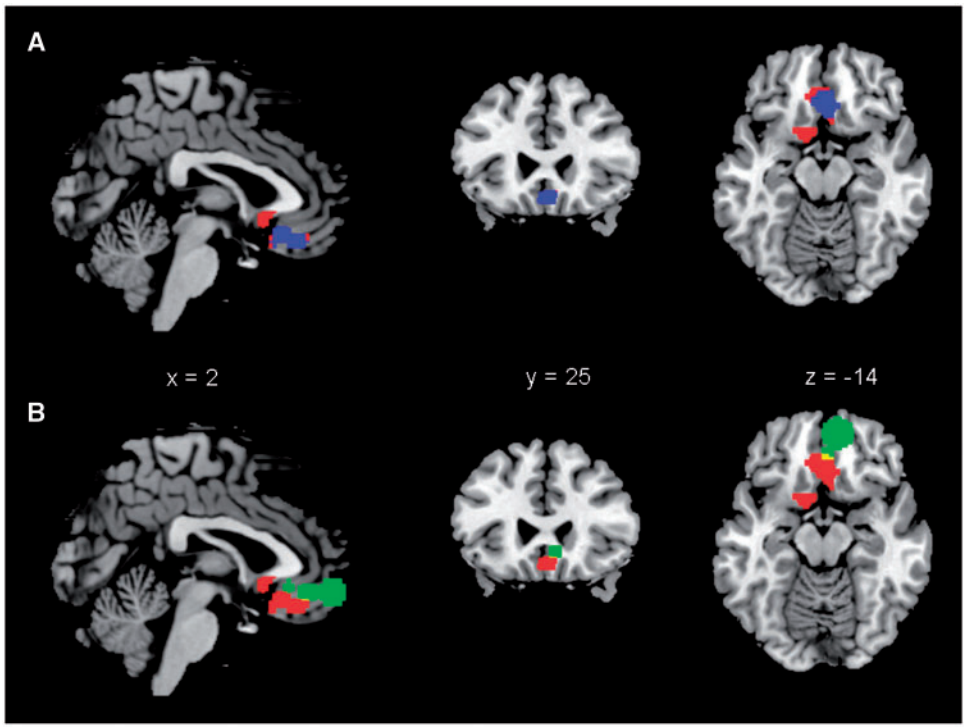

Fig. 3 The anatomical relationship between the vmPFC identified in the current study and brain regions identified in earlier studies that negatively correlated with SCL or positively correlated with SCR (Table 1). Only regions with MNI coordinate $z < 0$ were included. (**A**) Our vmPFC (red) overlaps brain regions negatively correlated with SCL during biofeedback (Nagai *et al.*, 2004) and resting state (Fan *et al.*, 2012). Blue color represents an area that overlapped across all studies. (**B**) Our vmPFC (red) show little overlap (yellow) with brain regions (green, combined from all studies) positively correlated with SCR. Anatomical boundary of the brain regions identified from the other studies was manually drawn according to the figures, coordinates and number of voxels reported.

area of the medial prefrontal cortex that involves both the anterior and posterior parts of the vmPFC and rostral/dACC. Given that activity of the rostral/dACC correlates positively with the SCR and plays a potential role in the generation of skin conductance (Critchley *et al.*, 2000), lesioning of this and adjacent structures could lead to impaired arousal. As selective lesions of these neighboring brain regions are rare, experimental lesioning of these specific areas in non-human primates may be required to pursue this issue.

Potential implications for clinical neuroscience

An increasing number of neuroimaging studies that sought to identify the brain anomalies associated with mood and anxiety disorders have implicated the vmPFC and neural circuits involving vmPFC (Savitz and Drevets, 2009; Hamani *et al.*, 2011; Myers-Schulz and Koenigs, 2012). Increased blood flow or metabolism of the subgenual ACC (sgACC)—a part of the posterior vmPFC—together with gray matter volume loss in this region, is a well-replicated finding in major depression (Savitz and Drevets, 2009). Deep brain stimulation of the sgACC ameliorates depressive symptoms in treatment-resistant patients (Drevets *et al.*, 2008; Holtzheimer *et al.*, 2012). FMRI studies presented a more diverse picture of vmPFC activity, depending on behavioral tasks, models and contrasts, as well as genotypes, patient populations and medication status (Keedwell *et al.*, 2005; Johnstone *et al.*, 2007; O'Nions *et al.*, 2011; Holsen *et al.*, 2012; Tao *et al.*, 2012). For instance, during evaluation of emotional words, depression patients showed a decreased response to negative compared with positive stimuli in the anterior vmPFC (Brassen *et al.*, 2008). Moreover, this altered pattern was positively correlated with symptom severity and 'normalized', accompanied by a significant improvement in symptoms, after treatment. It is posited that vmPFC participates in an extended 'visceromotor network' of structures that modulates autonomic/neuroendocrine responses during the neural processing of reward, fear and stress (Drevets *et al.*, 2008). Thus, the current finding of vmPFC regulation of physiological arousal adds an important dimension to this empirical literature.

Regulation of arousal: other brain regions and vmPFC connectivity

Amygdala is another key region involved in regulating electrodermal response (Phelps *et al.*, 2001; Williams *et al.*, 2001, 2005; Spoormaker *et al.*, 2011). Sweat responses failed to be evoked in a female patient with bilateral amygdala lesions caused by idiopathic encephalitis (Asahina *et al.*, 2003). Numerous non-human and human studies indicated that the vmPFC is both functionally and anatomically connected with the amygdala (Milad and Quirk, 2002; Ghashghaei *et al.*, 2007; Hare *et al.*, 2008; Myers-Schulz and Koenigs, 2012). A recent study of diffusion tensor imaging showed that the structural integrity of the pathway between the amygdala and vmPFC was inversely correlated with trait anxiety levels across subjects (Kim and Whalen, 2009). Although vmPFC control of amygdala activity is posited as a pathway to regulate physiological arousal and affect, the pattern of activations and functional connectivities seems to show a more complicated pattern of interaction between the two areas (Ochsner and Gross, 2005; Li *et al.*, 2009; Burghy *et al.*, 2012). Furthermore, midbrain and limbic structures other than the amygdala respond to salient stimuli and interact with the vmPFC to sustain an optimal level of physiological arousal for cognitive control (Brooks *et al.*, 2012; Sara and Bouret, 2012; Szabadi, 2012). It remains a challenge to understand the complexity of this interaction.

Methodological considerations

One potential issue concerns whether the SCR function (SCRF) and HRF are close enough, particularly in their latency, as suggested by previous studies (Patterson *et al.*, 2002; Nagai *et al.*, 2004), so that one can apply time series analyses such as correlation as well as GCA to these signals. More work clearly needs to be done to address this issue. On the other hand, previous studies have correlated BOLD and skin conductance time series with similar results, on the basis of this assumption (Patterson *et al.*, 2002; Nagai *et al.*, 2004). Furthermore, the latencies of SCRF derived in previous studies (Lim *et al.*, 1997; Alexander *et al.*, 2005; Bach *et al.*, 2010; Boucsein, 2011) were all close to and minimally faster than HRF. If the current finding of Granger causality were determined by the latency difference, we would have observed an opposite direction of causality.

It has also been questioned whether skin conductance could be used to quantify changes in sympathetic nerve activity since the relationship between skin conductance and sudomotor activity is non-linear (Kirno *et al.*, 1991). Direct recordings of skin sympathetic nerve activity (SSNA) with participants exposed to arousing visual images showed that, while the increases in SSNA were often coupled with sweat release and cutaneous vasoconstriction, these markers were not always consistent with the SSNA increases (Brown *et al.*, 2012). Concurrent brain imaging demonstrated that, during increases in SSNA, BOLD signals intensified in the central and lateral amygdala, dorsolateral pons, thalamus, nucleus accumbens and cerebellar cortex and decreased in the left orbitofrontal, frontal and right precuneus cortices (Henderson *et al.*, 2012). The pattern of brain activations overlapped but was not identical in association with SSNA and electrodermal response. Thus, it would be important to examine the role of the vmPFC in regulating physiological arousal by directly recording SSNA in future work.

Conclusions

To conclude, we reported a direct regulatory relationship between the activity of the vmPFC and skin conductance as a physiological index of arousal. Future work is warranted to investigate how this regulatory process may be compromised in patients with anxiety and mood disorders.

Conflict of Interest

None declared.

REFERENCES

Abler, B., Roebroeck, A., Goebel, R., et al. (2006). Investigating directed influences between activated brain areas in a motor-response task using fMRI. *Magnetic Resonance Imaging*, *24*(2), 181–5.

Alexander, D.M., Trengove, C., Johnston, P., Cooper, T., August, J.P., Gordon, E. (2005). Separating individual skin conductance responses in a short interstimulus-interval paradigm. *Journal of Neuroscience Methods*, *146*(1), 116–23.

Asahina, M., Suzuki, A., Mori, M., Kanesaka, T., Hattori, T. (2003). Emotional sweating response in a patient with bilateral amygdala damage. *International Journal of Psychophysiology*, *47*(1), 87–93.

Ashburner, J., Friston, K.J. (1999). Nonlinear spatial normalization using basis functions. *Human Brain Mapping*, *7*(4), 254–66.

Bach, D.R., Flandin, G., Friston, K.J., Dolan, R.J. (2010). Modelling event-related skin conductance responses. *International Journal of Psychophysiology*, *75*(3), 349–56.

Bechara, A., Damasio, H., Tranel, D., Damasio, A.R. (1997). Deciding advantageously before knowing the advantageous strategy. *Science*, *275*(5304), 1293–5.

Boucsein, W. (2011). *Electrodermal Activity*. New York: Springer.

Brassen, S., Kalisch, R., Weber-Fahr, W., Braus, D.F., Buchel, C. (2008). Ventromedial prefrontal cortex processing during emotional evaluation in late-life depression: a longitudinal functional magnetic resonance imaging study. *Biological Psychiatry*, *64*(4), 349–55.

Brooks, S.J., Savov, V., Allzen, E., Benedict, C., Fredriksson, R., Schioth, H.B. (2012). Exposure to subliminal arousing stimuli induces robust activation in the amygdala, hippocampus, anterior cingulate, insular cortex and primary visual cortex: a systematic meta-analysis of fMRI studies. *Neuroimage*, *59*(3), 2962–73.

Brown, R., James, C., Henderson, L.A., Macefield, V.G. (2012). Autonomic markers of emotional processing: skin sympathetic nerve activity in humans during exposure to emotionally charged images. *Frontiers in Physiology*, *3*, 394.

Burghy, C.A., Stodola, D.E., Ruttle, P.L., et al. (2012). Developmental pathways to amygdala-prefrontal function and internalizing symptoms in adolescence. *Nature Neuroscience*, *15*(12), 1736–41.

Chao, H.H., Luo, X., Chang, J.L., Li, C.S. (2009). Activation of the pre-supplementary motor area but not inferior prefrontal cortex in association with short stop signal reaction time—an intra-subject analysis. *BMC Neuroscience*, *10*, 75.

Charles, F., Bond, J., Richardson, K. (2004). Seeing the fisher z-transformation. *Psychometrika*, *69*(2), 291–303.

Critchley, H.D. (2002). Electrodermal responses: what happens in the brain. *Neuroscientist*, *8*(2), 132–42.

Critchley, H.D. (2009). Psychophysiology of neural, cognitive and affective integration: fMRI and autonomic indicants. *International Journal of Psychophysiology*, *73*(2), 88–94.

Critchley, H.D., Elliott, R., Mathias, C.J., Dolan, R.J. (2000). Neural activity relating to generation and representation of galvanic skin conductance responses: a functional magnetic resonance imaging study. *Journal of Neuroscience*, *20*(8), 3033–40.

Critchley, H.D., Mathias, C.J., Dolan, R.J. (2001). Neural activity in the human brain relating to uncertainty and arousal during anticipation. *Neuron*, *29*(2), 537–45.

Damasio, A.R. (1994). *Descartes' Error: Emotion, Reason and the Human Brain*. New York: Putnam.

Damasio, A.R., Tranel, D., Damasio, H. (1990). Individuals with sociopathic behavior caused by frontal damage fail to respond autonomically to social stimuli. *Behavioural Brain Research*, *41*(2), 81–94.

Damasio, A.R., Tranel, D., Damasio, H.C. (1991). Somatic markers and the guidance of behavior: theory and preliminary testing. In: Levin, H.S., Eisenberg, H.M., Benton, L.B., editors. *Frontal Lobe Function and Dysfunction*. New York: Oxford University Press, pp. 217–29.

De Jong, R., Coles, M.G., Logan, G.D., Gratton, G. (1990). In search of the point of no return: the control of response processes. *Journal of Experimental Psychology. Human Perception and Performance*, *16*(1), 164–82.

Delgado, M.R., Nearing, K.I., Ledoux, J.E., Phelps, E.A. (2008). Neural circuitry underlying the regulation of conditioned fear and its relation to extinction. *Neuron*, *59*(5), 829–38.

Deshpande, G., Hu, X., Stilla, R., Sathian, K. (2008). Effective connectivity during haptic perception: a study using Granger causality analysis of functional magnetic resonance imaging data. *Neuroimage*, *40*(4), 1807–14.

Deshpande, G., LaConte, S., James, G.A., Peltier, S., Hu, X. (2009). Multivariate Granger causality analysis of fMRI data. *Human Brain Mapping*, *30*(4), 1361–73.

Ding, M., Bressler, S.L., Yang, W., Liang, H. (2000). Short-window spectral analysis of cortical event-related potentials by adaptive multivariate autoregressive modeling: data preprocessing, model validation, and variability assessment. *Biological Cybernetics*, *83*(1), 35–45.

Ding, M., Chen, Y., Bressler, S.L. (2006). Granger causality: basic theory and application to neuroscience. In: Schelter, B., Winderhalder, M., Timmer, J., editors. *Handbook of Time Series Analysis*. Berlin: Wiley-VCH, pp. 451–74.

Dolan, R.J. (2002). Emotion, cognition, and behavior. *Science*, *298*(5596), 1191–4.

Drevets, W.C., Price, J.L., Simpson, J.R., Jr, et al. (1997). Subgenual prefrontal cortex abnormalities in mood disorders. *Nature*, *386*(6627), 824–7.

Drevets, W.C., Savitz, J., Trimble, M. (2008). The subgenual anterior cingulate cortex in mood disorders. *CNS Spectrums*, *13*(8), 663–81.

Duann, J.R., Ide, J.S., Luo, X., Li, C.S. (2009). Functional connectivity delineates distinct roles of the inferior frontal cortex and presupplementary motor area in stop signal inhibition. *Journal of Neuroscience*, *29*(32), 10171–9.

Fan, J., Xu, P., Van Dam, N.T., et al. (2012). Spontaneous brain activity relates to autonomic arousal. *Journal of Neuroscience*, *32*(33), 11176–86.

Figner, B., Murphy, R.O. (2011). Using skin conductance in judgment and decision making research. In: Schulte-Mecklenbeck, M., Kuehberger, A., Ranyard, R., editors. *A Handbook of Process Tracing Methods for Decision Research*. New York: Psychology Press, pp. 163–84.

First, M.B., Spitzer, R.L., Williams, J.B.W., Gibbon, M. (1995). *Structured Clinical Interview for DSM-IV (SCID)*. Washington, DC: American Psychiatric Association.

Fox, M.D., Snyder, A.Z., Vincent, J.L., Corbetta, M., Van Essen, D.C., Raichle, M.E. (2005). The human brain is intrinsically organized into dynamic, anticorrelated functional networks. *Proceedings of the National Academy of Sciences of the United States of America*, *102*(27), 9673–8.

Frith, C.D., Allen, H.A. (1983). The skin conductance orienting response as an index of attention. *Biological Psychology*, *17*(1), 27–39.

Gentle, J.E., Härdle, W., Mori, Y. (2004). *Handbook of Computational Statistics: Concepts and Methods*. Berlin: Springer.

Ghashghaei, H.T., Hilgetag, C.C., Barbas, H. (2007). Sequence of information processing for emotions based on the anatomic dialogue between prefrontal cortex and amygdala. *Neuroimage*, *34*(3), 905–23.

Gianaros, P.J., Horenstein, J.A., Cohen, S., et al. (2007). Perigenual anterior cingulate morphology covaries with perceived social standing. *Social Cognitive and Affective Neuroscience*, *2*(3), 161–73.

Glascher, J., Hampton, A.N., O'Doherty, J.P. (2009). Determining a role for ventromedial prefrontal cortex in encoding action-based value signals during reward-related decision making. *Cerebral Cortex*, *19*(2), 483–95.

Granger, C.W.J. (1969). Investigating causal relations by econometric models and cross-spectral methods. *Econometrica*, *37*, 424.

Greicius, M.D., Flores, B.H., Menon, V., et al. (2007). Resting-state functional connectivity in major depression: abnormally increased contributions from subgenual cingulate cortex and thalamus. *Biological Psychiatry*, *62*(5), 429–37.

Hamani, C., Mayberg, H., Stone, S., Laxton, A., Haber, S., Lozano, A.M. (2011). The subcallosal cingulate gyrus in the context of major depression. *Biological Psychiatry*, *69*(4), 301–8.

Hamilton, J.D. (1994). *Time Series Analysis*. Princeton, NJ: Princeton University Press.

Hare, T.A., Tottenham, N., Galvan, A., Voss, H.U., Glover, G.H., Casey, B.J. (2008). Biological substrates of emotional reactivity and regulation in adolescence during an emotional go-nogo task. *Biological Psychiatry*, *63*(10), 927–34.

Harrison, L., Penny, W.D., Friston, K. (2003). Multivariate autoregressive modeling of fMRI time series. *Neuroimage*, *19*(4), 1477–91.

Henderson, L.A., Stathis, A., James, C., Brown, R., McDonald, S., Macefield, V.G. (2012). Real-time imaging of cortical areas involved in the generation of increases in skin sympathetic nerve activity when viewing emotionally charged images. *Neuroimage*, *62*(1), 30–40.

Holsen, L.M., Lee, J.H., Spaeth, S.B., et al. (2012). Brain hypoactivation, autonomic nervous system dysregulation, and gonadal hormones in depression: a preliminary study. *Neuroscience Letters*, *514*(1), 57–61.

Holtzheimer, P.E., Kelley, M.E., Gross, R.E., et al. (2012). Subcallosal cingulate deep brain stimulation for treatment-resistant unipolar and bipolar depression. *Archives of General Psychiatry*, *69*(2), 150–8.

Ide, J.S., Li, C.S. (2011a). A cerebellar thalamic cortical circuit for error-related cognitive control. *Neuroimage*, *54*(1), 455–64.

Ide, J.S., Li, C.S. (2011b). Error-related functional connectivity of the habenula in humans. *Frontiers in Human Neuroscience*, *5*, 25.

Johnstone, T., van Reekum, C.M., Urry, H.L., Kalin, N.H., Davidson, R.J. (2007). Failure to regulate: counterproductive recruitment of top-down prefrontal-subcortical circuitry in major depression. *Journal of Neuroscience*, *27*(33), 8877–84.

Keedwell, P.A., Andrew, C., Williams, S.C., Brammer, M.J., Phillips, M.L. (2005). The neural correlates of anhedonia in major depressive disorder. *Biological Psychiatry*, *58*(11), 843–53.

Kennedy, S.H., Konarski, J.Z., Segal, Z.V., et al. (2007). Differences in brain glucose metabolism between responders to CBT and venlafaxine in a 16-week randomized controlled trial. *American Journal of Psychiatry*, *164*(5), 778–88.

Kim, H., Shimojo, S., O'Doherty, J.P. (2010). Overlapping responses for the expectation of juice and money rewards in human ventromedial prefrontal cortex. *Cerebral Cortex*, *21*(4), 769–76.

Kim, M.J., Whalen, P.J. (2009). The structural integrity of an amygdala-prefrontal pathway predicts trait anxiety. *Journal of Neuroscience*, *29*(37), 11614–8.

Kirno, K., Kunimoto, M., Lundin, S., Elam, M., Wallin, B.G. (1991). Can galvanic skin response be used as a quantitative estimate of sympathetic nerve activity in regional anesthesia? *Anesthesia and Analgesia*, *73*(2), 138–42.

Levitt, H. (1971). Transformed up-down methods in psychoacoustics. *The Journal of the Acoustical Society of America*, *49*(2), 467+.

Li, C.S., Chao, H.H., Lee, T.W. (2009). Neural correlates of speeded as compared with delayed responses in a stop signal task: an indirect analog of risk taking and association with an anxiety trait. *Cerebral Cortex*, *19*(4), 839–48.

Lim, C.L., Rennie, C., Barry, R.J., et al. (1997). Decomposing skin conductance into tonic and phasic components. *Int J Psychophysiol*, *25*(2), 97–109.

Masten, C.L., Eisenberger, N.I., Borofsky, L.A., et al. (2009). Neural correlates of social exclusion during adolescence: understanding the distress of peer rejection. *Social Cognitive and Affective Neuroscience*, *4*(2), 143–57.

Mayberg, H.S., Brannan, S.K., Tekell, J.L., et al. (2000). Regional metabolic effects of fluoxetine in major depression: serial changes and relationship to clinical response. *Biological Psychiatry*, *48*(8), 830–43.

Mayberg, H.S., Lozano, A.M., Voon, V., et al. (2005). Deep brain stimulation for treatment-resistant depression. *Neuron*, *45*(5), 651–60.

Milad, M.R., Quirk, G.J. (2002). Neurons in medial prefrontal cortex signal memory for fear extinction. *Nature*, *420*(6911), 70–4.

Milad, M.R., Wright, C.I., Orr, S.P., Pitman, R.K., Quirk, G.J., Rauch, S.L. (2007). Recall of fear extinction in humans activates the ventromedial prefrontal cortex and hippocampus in concert. *Biological Psychiatry*, *62*(5), 446–54.

Myers-Schulz, B., Koenigs, M. (2012). Functional anatomy of ventromedial prefrontal cortex: implications for mood and anxiety disorders. *Molecular Psychiatry*, *17*(2), 132–41.

Nagai, Y., Critchley, H.D., Featherstone, E., Trimble, M.R., Dolan, R.J. (2004). Activity in ventromedial prefrontal cortex covaries with sympathetic skin conductance level: a physiological account of a "default mode" of brain function. *Neuroimage*, *22*(1), 243–51.

Naqvi, N.H., Bechara, A. (2006). Skin conductance: a psychophysiological approach to the study of decision making. In: Senior, C., Russell, T., Gazzaniga, M.S., editors. *Methods in Mind*. Cambridge, MA, US: The MIT Press, pp. 103–22.

Nili, U., Goldberg, H., Weizman, A., Dudai, Y. (2010). Fear thou not: activity of frontal and temporal circuits in moments of real-life courage. *Neuron*, *66*(6), 949–62.

O'Nions, E.J., Dolan, R.J., Roiser, J.P. (2011). Serotonin transporter genotype modulates subgenual response to fearful faces using an incidental task. *J Cogn Neurosci*, *23*(11), 3681–93.

Ochsner, K.N., Gross, J.J. (2005). The cognitive control of emotion. *Trends in Cognitive Science*, *9*(5), 242–9.

Paradiso, S., Robinson, R.G., Boles Ponto, L.L., Watkins, G.L., Hichwa, R.D. (2003). Regional cerebral blood flow changes during visually induced subjective sadness in healthy elderly persons. *J Neuropsychiatry Clin Neurosci*, *15*(1), 35–44.

Patterson, J.C. 2nd Ungerleider, L.G., Bandettini, P.A. (2002). Task-independent functional brain activity correlation with skin conductance changes: an fMRI study. *Neuroimage*, *17*(4), 1797–806.

Penny, W.D., Holmes, A.P., Friston, K. (2004). Random-effects analysis. In: Frackowiak, R., Frith, C., Dolan, R.J. et al. editors. *Human Brain Function*. San Diego, California, US: Academic Press, pp. 843–50.

Phelps, E.A., O'Connor, K.J., Gatenby, J.C., Gore, J.C., Grillon, C., Davis, M. (2001). Activation of the left amygdala to a cognitive representation of fear. *Nature Neuroscience*, *4*(4), 437–41.

Roebroeck, A., Formisano, E., Goebel, R. (2005). Mapping directed influence over the brain using Granger causality and fMRI. *Neuroimage*, *25*(1), 230–42.

Sara, S.J., Bouret, S. (2012). Orienting and reorienting: the locus coeruleus mediates cognition through arousal. *Neuron*, *76*(1), 130–41.

Sato, J.R., Takahashi, D.Y., Arcuri, S.M., Sameshima, K., Morettin, P.A., Baccala, L.A. (2009). Frequency domain connectivity identification: an application of partial directed coherence in fMRI. *Human Brain Mapping*, *30*(2), 452–61.

Savitz, J.B., Drevets, W.C. (2009). Imaging phenotypes of major depressive disorder: genetic correlates. *Neuroscience*, *164*(1), 300–30.

Schiller, D., Levy, I., Niv, Y., LeDoux, J.E., Phelps, E.A. (2008). From fear to safety and back: reversal of fear in the human brain. *Journal of Neuroscience*, *28*(45), 11517–25.

Schwarz, G. (1978). Estimating the dimension of a model. *Annals of Statistics*, *6*(2), 461–4.

Seth, A.K. (2010). A MATLAB toolbox for Granger causal connectivity analysis. *Journal of Neuroscience Methods*, *186*(2), 262–73.

Simpson, J.R., Jr, Drevets, W.C., Snyder, A.Z., Gusnard, D.A., Raichle, M.E. (2001). Emotion-induced changes in human medial prefrontal cortex: II. During anticipatory anxiety. *Proceedings of the National Academy of Sciences of the United States of America*, *98*(2), 688–93.

Somerville, L.H., Heatherton, T.F., Kelley, W.M. (2006). Anterior cingulate cortex responds differentially to expectancy violation and social rejection. *Nature Neuroscience*, *9*(8), 1007–8.

Somerville, L.H., Kelley, W.M., Heatherton, T.F. (2010). Self-esteem modulates medial prefrontal cortical responses to evaluative social feedback. *Cerebral Cortex*, *20*(12), 3005–13.

Spoormaker, V.I., Andrade, K.C., Schroter, M.S., et al. (2011). The neural correlates of negative prediction error signaling in human fear conditioning. *Neuroimage*, *54*(3), 2250–6.

Stilla, R., Deshpande, G., LaConte, S., Hu, X., Sathian, K. (2007). Posteromedial parietal cortical activity and inputs predict tactile spatial acuity. *Journal of Neuroscience*, *27*(41), 11091–102.

Szabadi, E. (2012). Modulation of physiological reflexes by pain: role of the locus coeruleus. *Frontiers in Integrative Neuroscience*, *6*, 94.

Tao, R., Calley, C.S., Hart, J., et al. (2012). Brain activity in adolescent major depressive disorder before and after fluoxetine treatment. *American Journal of Psychiatry*, *169*(4), 381–8.

Tranel, D., Damasio, H. (1994). Neuroanatomical correlates of electrodermal skin conductance responses. *Psychophysiology*, *31*(5), 427–38.

Wen, X., Yao, L., Liu, Y., Ding, M. (2012). Causal interactions in attention networks predict behavioral performance. *Journal of Neuroscience*, *32*(4), 1284–92.

Williams, L.M., Das, P., Liddell, B., et al. (2005). BOLD, sweat and fears: fMRI and skin conductance distinguish facial fear signals. *Neuroreport*, *16*(1), 49–52.

Williams, L.M., Phillips, M.L., Brammer, M.J., et al. (2001). Arousal dissociates amygdala and hippocampal fear responses: evidence from simultaneous fMRI and skin conductance recording. *Neuroimage*, *14*(5), 1070–9.

Zahn, T.P., Grafman, J., Tranel, D. (1999). Frontal lobe lesions and electrodermal activity: effects of significance. *Neuropsychologia*, *37*(11), 1227–41.

Zald, D.H., Mattson, D.L., Pardo, J.V. (2002). Brain activity in ventromedial prefrontal cortex correlates with individual differences in negative affect. *Proceedings of the National Academy of Sciences of the United States of America*, *99*(4), 2450–4.

Zhang, S., Hu, S., Chao, H.H., Luo, X., Farr, O.M., Li, C.S. (2012). Cerebral correlates of skin conductance responses in a cognitive task. *Neuroimage*, *62*(3), 1489–98.

Zhang, S., Li, C.S. (2012a). Functional networks for cognitive control in a stop signal task: Independent component analysis. *Human Brain Mapping*, *33*(1), 89–104.

Zhang, S., Li, C.S. (2012b). Functional connectivity mapping of the human precuneus by resting state fMRI. *Neuroimage*, *59*(4), 3548–62.